Communications in Nonlinear Science and Numerical Simulation 120 (2023) 107184

Contents lists available at ScienceDirect

Communications in Nonlinear Science and Numerical Simulation

journal homepage: www.elsevier.com/locate/cnsns

Research paper

Controlling the bursting size in the two-dimensional Rulkov model

Jennifer López [a], Mattia Coccolo [a,*], Rubén Capeáns [a], Miguel A.F. Sanjuán [a,b]

[a] Nonlinear Dynamics, Chaos and Complex Systems Group, Departamento de Física, Universidad Rey Juan Carlos, Tulipán s/n, 28933 Móstoles, Madrid, Spain

[b] Department of Applied Informatics, Kaunas University of Technology, Studentu 50-415, Kaunas LT-51368, Lithuania

ARTICLE INFO

Article history:
Received 14 July 2022
Received in revised form 16 January 2023
Accepted 16 February 2023
Available online 20 February 2023

Keywords:
Control of chaos
Rulkov
Neuron
Transient chaos

ABSTRACT

We propose to control the orbits of the two-dimensional Rulkov model affected by bounded noise. For the correct parameter choice the phase space presents two chaotic regions separated by a transient chaotic region in between. One of the chaotic regions is the responsible to give birth to the neuronal bursting regime. Normally, an orbit in this chaotic region cannot pass through the transient chaotic one and reach the other chaotic region. As a consequence the burstings are short in time. Here, we propose a control technique to connect both chaotic regions and allow the neuron to exhibit very long burstings. This control method defines a region Q covering the transient chaotic region where it is possible to find an advantageous set $S \subset Q$ through which the orbits can be driven with a minimal control. In addition we show how the set S changes depending on the noise intensity affecting the map, and how the set S can be used in different scenarios of control.

1. Introduction

Neurons are complex entities that form a highly structured network. In recent decades, it has been of interest to create mathematical models that mimic their behaviour. Due to their high complexity, these models have to be approximated and simplified while retaining only certain functionalities of the neurons. The entire structure of the neuron is usually replaced by a system with a voltage membrane and a connection topology.

Initially, continuous models such as the models of FitzHugh–Nagumo [1], Hindmarsh-Rose [2], and Hodgkin–Huxley [3] have been used profusely. Recently, discrete models have started to arouse interest for the simulation of neurons [4]. They are easier models to solve (they avoid the integration of ordinary differential equations), and they are able to produce a wide range of dynamical behaviour like periodic oscillations, spiking and chaotic bursting. In this context, it is common to use two-dimensional maps of the slow–fast type variables (fast–slow system). The most relevant are [4]: the Izhikevich's discrete model, Courbage's model, Chialvo's model, and the Rulkov model. The latter presents three variants of the model: non-chaotic, supercritical, and chaotic.

The chaotic Rulkov neuron map [5–11] is used in this work, because it is a simple model that can exhibit the basic regimes of neuronal activity, as rest, bursts, spikes, with the last two allowing periodic and chaotic dynamics. The use of this simple map is intended to demonstrate the application of our control algorithm and we will show in Section 7 how the method can be applied in other maps. In this work, we focus our attention in the regime where the Rulkov map

* Corresponding author.
E-mail address: mattiatommaso.coccolo@urjc.es (M. Coccolo).

https://doi.org/10.1016/j.cnsns.2023.107184

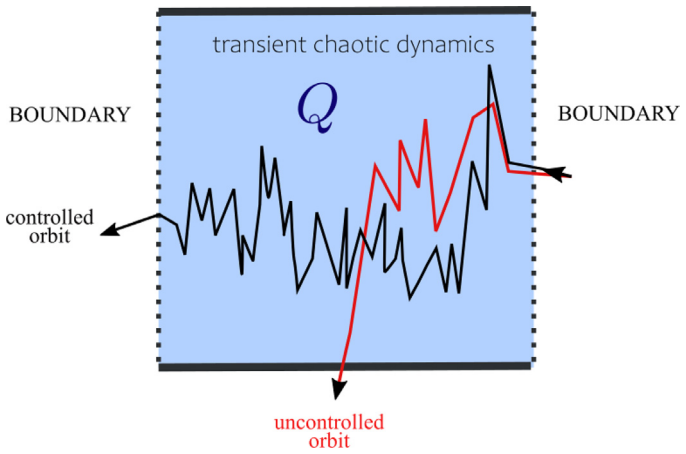

Fig. 1. Control goal. Q is a region in the phase space previously defined by the controller. In absence of control, an orbit (red orbit) enters in Q through the right boundary (right dashed line) but never reaches the left boundary (left dashed line), since it abandons Q through the bottom boundary. With the suitable application of control it is possible to sustain the orbit (black orbit) in Q until it reaches the right boundary. In this way, the region Q acts as a pathway for the controlled orbits, connecting different parts of the phase space.

exhibits bursting. They are cycles of rapid action potential spiking followed by quiescent periods much longer than typical inter-spike intervals. In this model these cycles alternate high activity of the neuron exhibiting fast chaotic oscillations (the bursts), together with time periods of low activity without chaotic motion. Typically the bursting size (time interval of bursting) is short because these chaotic oscillations takes place in a narrow chaotic region of the phase space delimited by the presence of an unstable manifold. Once the chaotic orbit touches this unstable manifold the bursting rapidly extinguished giving way to a low activity period.

However, we found that it is possible to greatly increase the bursting size of the neuron exploiting the fact that there is a second chaotic region in the phase space. This second chaotic region is separated from the main chaotic region, where the bursting of the neuron takes place. In this work we explore the possibility to built a path in the phase space connecting both chaotic regions, allowing the chaotic orbits to pass from one to another, and therefore extending or adjusting the size of the burstings. The potential application of this control, lies in the crucial role that neural burst firing patterns play in the encoding and transmission of specific information [12,13] and for the operation of the central pattern generators (CPGs) [14,15], responsible for essential rhythmic behaviours such as walking or breathing. Additionally, abnormal firing is implicated in a series of neural pathologies [16], such as epilepsy [17,18]. Therefore, controlling the bursting size can help to prevent these abnormal firing patterns.

To reach our goal, we present a control method inspired in our previous work of partial control [19–25] that also takes into account noise affecting the system, as in all real systems. This method is applied on maps in which the variables are assumed to be accessible for control. The region in the phase space where the orbits are controlled is called Q. In this work this region Q is located between both chaotic regions. Through a recursive algorithm that we will show in the following sections, it can be computed a special subset called $S \subset Q$ through which the orbits can be controlled to go from one chaotic region to the other, minimizing the need of control. Furthermore we will see that this method adapts to the intensity of noise affecting the map. Different intensities result in different sets S.

Although this control method resembles the partial control method and they share similarities in the steps to apply it, we want to emphasize that there is a substantial difference in the control goal. While partial control is designed to keep the orbits forever in the region Q of the phase space, this control method is designed to steer the orbits through the region Q, allowing the orbits to enter or abandon it via a portion of its boundaries, previously set by the controller, as it is shown schematically in Fig. 1. This control method is specially indicated to connect different regions of phase space that otherwise would be isolated .

The manuscript is organized as follows. In Section 2, we introduce the model system. In Section 3, we describe the control technique. Then, in Sections 4 and 5, we apply the control technique to the system in different scenarios, where we also show results for different noise intensities to illustrate how the set S changes. In Section 6 we discuss the results when one of the variables is not controlled or affected by the noise. In Section 7 we discuss how to generalize the method to other systems. Finally, in Section 8 we summarize the main results of the paper.

2. The two-dimensional Rulkov map

The chaotic Rulkov model [5–8] is a two-dimensional map that achieves to exhibit the basic regimes of neuronal activity with a simple model.

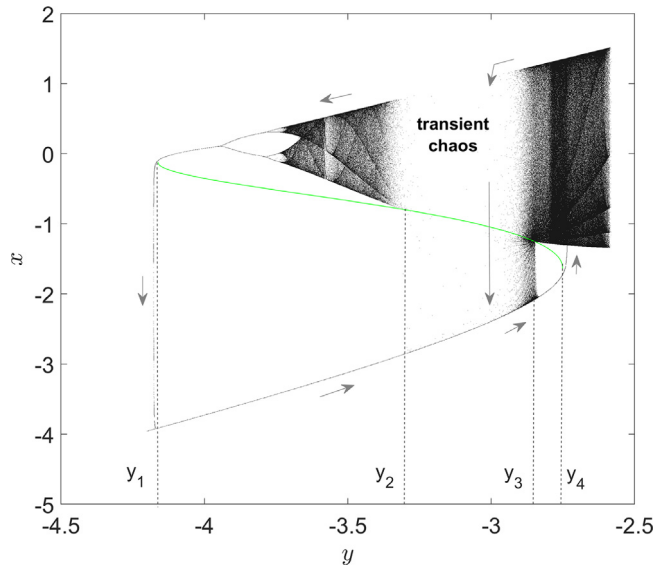

Fig. 2. Behaviour of the orbits in the Rulkov map. Here, we take an uniform grid of 1623 × 2739 initial conditions in the rectangle $(y, x) \in [-4.5, -2.5] \times [-5, 2]$. For each initial condition we compute 100 iterations of the corresponding orbit, computed with Eq. (1). We only show the iteration 100th to avoid the fast transient and visualize the separated right and left chaotic regions. Notice that this is not a bifurcation diagram since the y value also change in every iteration of the orbit. However as y is the slow variable, it behaves almost like a parameter and that is the reason the figure resembles a bifurcation diagram. The small arrows displayed, indicate the average motion of the orbits in each region of the phase space.

The equations of the system are:

$$\begin{aligned} x_{n+1} &= \frac{\alpha}{(1+x_n^2)} + y_n \\ y_{n+1} &= y_n - \sigma x_n - \beta, \end{aligned} \tag{1}$$

being x the voltage of the neuron membrane (taking the role of the fast variable), and y the ion concentration (representing the slow variable) where α, σ and β are the system parameters. Here we are interested in the regime where the system exhibits chaotic oscillations [26], so we fix the values $\alpha = 4.1$, $\sigma = \beta = 0.001$, following Rulkov's original article [5].

The behaviour of the orbits in the phase space is shown in Fig. 2. At first glance, the figure looks like a bifurcation diagram but that is not the case. In Eq. (1), both variables x and y are changing. However the change of the y variable is so slow in comparison with the variable x, that it behaves almost as a parameter, and that is why the orbits in the phase space, shown in Fig. 2, resembles a bifurcation diagram.

To build Fig. 2, we took a grid of initial conditions in the rectangle $(y, x) \in [-4.5, -2.5] \times [-5, 2]$ and for each initial condition we simulate 100 iterations of the corresponding orbit. We remove the first 99 iterations and we display the iteration 100. In this way, we can synthesize and obtain qualitative information about the behaviour of the orbits in the phase space. The number 99 is just a choice. Taking a slightly higher or lower number does not significantly alter the visual appearance of the figure where it can be appreciated the diversity in the dynamics that offers this system. In fact, it is possible to discern how the trajectories can become chaotic between y_1 and y_2, a periodic region between y_2 and y_3, then, again, a chaotic region beyond y_3. Worth to mention are the stable (in black) and unstable (in green) manifolds between y_1 and y_4. The mentioned (y_1, y_2, y_3, y_4) important points are indicated in the figure. At points y_1 and y_4, the stable an unstable manifold (displayed in green) intersects, and therefore the orbits changes their stability. Between the points y_2 and y_3, transient chaotic dynamics takes place. Orbits in this region quickly decay below the unstable manifold and reach the bottom stable manifold.

To explain how the orbits behave in the phase space (see Fig. 2), let us take an orbit starting in some point on the left chaotic region ($y < y_2$). Here the orbit quickly oscillates in the vertical axis (x-axis) while it slowly moves to the left (y-axis) towards the periodic region where, eventually, it reaches the point ($y = y_1$). At this point, the orbits touch the unstable manifold and fall to the stable manifold at the bottom. Here the orbits starts to move to the right along the stable manifold until it reaches the value ($y = y_4$), where the orbits meet again the unstable manifold and jumps to the right chaotic region at the top. In this region the orbit starts to oscillate chaotically, while it slowly moves to the left. Finally the orbit reaches the crisis point ($y = y_3$), and it falls again in the bottom stable manifold, repeating forever the chaotic cycle around the values y_3 and y_4. So, we define the beginning of a burst when the trajectory touches y_4 and the end when it falls on the stable manifold between y_2 and y_3.

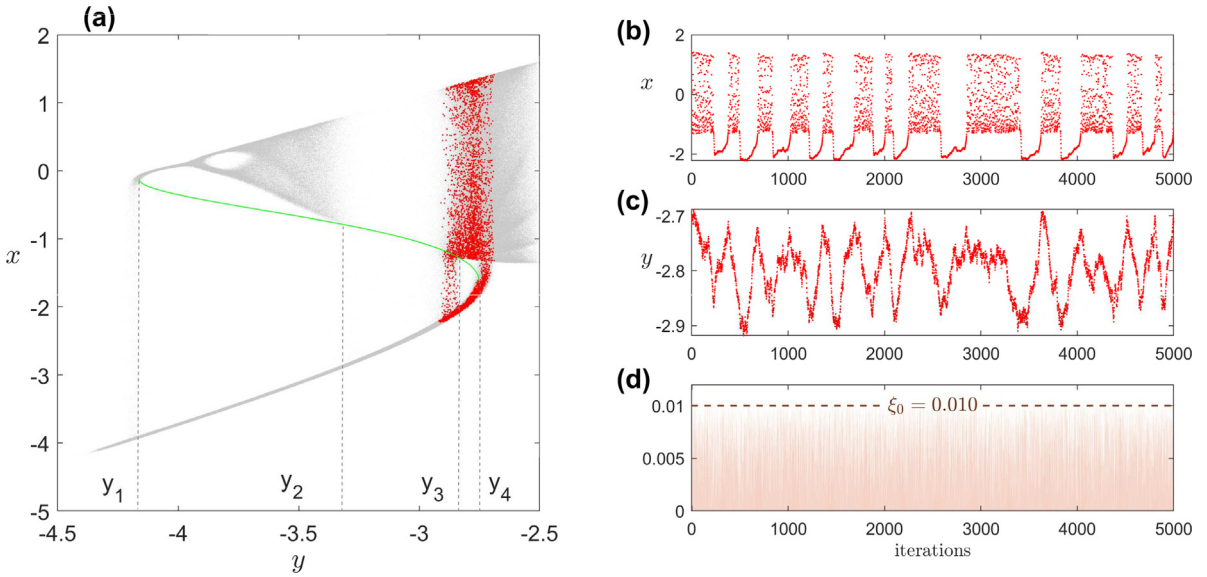

Fig. 3. Chaotic cycle affected by disturbances. (a) The background orbits shown in grey have been computed in the same way as Fig. 2 but instead, these orbits correspond with Eq. (2) where an upper bound of disturbance $\xi_0 = 0.010$ has been taken. Eventually all these orbits converges to the chaotic cycle (red dots) that remains confined around y_3 and y_4. The orbit displayed consists of 5000 iterations and the corresponding x (fast variable) and y (slow variable) time series of the red orbit are shown in (b) and (c) respectively. In (d) the disturbances $|\xi_n| \leq \xi_0$ affecting the orbit.

To model a more real behaviour of the neuron, we consider that Eq. (1) are affected by some additive bounded noise, that we call disturbance. In the literature, we can find authors that consider the disturbance affecting only the fast variable x [6,8]. Others consider the disturbance affecting the slow variable y [27] and others consider a disturbance affecting both variables [7,28,29]. In this work, we consider this last case for being the most general, and at the end of the paper we analyse the particular cases of the disturbance affecting only one variable. The Rulkov map affected by a disturbance is given by:

$$\begin{aligned} x_{n+1} &= \frac{\alpha}{(1+x_n^2)} + y_n + \xi_n^x \\ y_{n+1} &= y_n - \sigma x_n - \beta + \xi_n^y, \end{aligned} \tag{2}$$

where ξ_n^x and ξ_n^y are the disturbances on each variable. Physically, the disturbance in x can represent, for example, the synaptic input noise in the neuron membrane voltage, while the disturbance in y models ion-concentration fluctuations, which may be either from outside the cell or from inside [30]. The only condition that we impose is that the disturbance is bounded as $\sqrt{(\xi_n^x)^2 + (\xi_n^y)^2} \leq \xi_0$. In this way, we are confident that it does not become too large compared to the orbits.

The behaviour of the noisy orbits in the Rulkov map given by Eq. (2) is displayed in Fig. 3. In grey we display many orbits in the phase space taking a grid of initial conditions in the rectangle $(y, x) \in [-4.5, -2.5] \times [-5, 2]$. The grey orbits have been computed in the same way as the orbits displayed Fig. 2 but using instead the Eq. (2) with an upper disturbance bound $\xi_0 = 0.010$. Eventually all these orbits end in the chaotic cycle displayed by the red dots. In the same figure, we also display the x and y time series corresponding to the chaotic cycle and the disturbances $|\xi_n| \leq \xi_0 = 0.010$ affecting it. Notice that due to the disturbances, the orbit can touch the unstable manifold before reaching the points y_3 and y_4, respectively, and therefore the bursting sizes are more irregular in comparison with the deterministic case ($\xi_0 = 0$), but yet short in time.

In this scenario, we propose a control technique to increase the bursting size taking advantage of the presence of the transient chaotic region between y_2 and y_3 and the left chaotic region. Normally, the chaotic cycles trapped in the right chaotic region could never reach the left chaotic region. However, with a suitable application of control it is possible to sustain the chaotic orbits in the transient chaotic region and allow them to reach the left chaotic region, extending the bursting size of the neuron as it is schematically draw in Fig. 4.

3. Control scheme

As shown in Fig. 4, when an orbit enters in the transient chaotic region, approximately $y_2 < y < y_3$, after a short transient, it touches the unstable manifold (green line) and fall towards the stable manifold at the bottom. To avoid this escape, we will apply control in the region Q defined as the rectangle $(y, x) \in [-3.42, -2.78] \times [-1.82, 1.92]$. This region

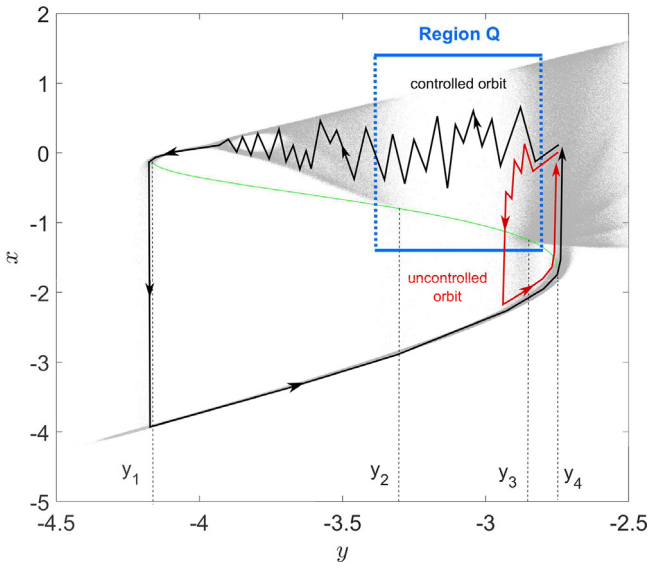

Fig. 4. Scheme of the control goal in the phase space of the Rulkov map. The background orbits shown in grey are the same as displayed in Fig. 3. They will also be displayed in other figures as a background reference to help the visualization of the uncontrolled and controlled orbits in the phase space. In red colour an uncontrolled orbit and in black a controlled one. Both are draw schematically. The control is applied in Q to sustain the transient chaotic orbit and allow it to complete a long bursting. The right and left sides of Q are defined as open boundaries (dashed blue lines) to allow the orbit to enter and escape from Q.

is y-wide enough to contain the interval $y_2 < y < y_3$, and x-wide enough to allow the chaotic oscillation of the fast variable x and therefore, preserving the dynamical behaviour of the burstings in this region.

In this control scheme, we consider the general case where the control is applied on both variables. At the end of the paper we particularize to the case where the control is only applied on only one variable. The Rulkov map with control in both variables is given by:

$$\begin{aligned} x_{n+1} &= \frac{\alpha}{(1+x_n^2)} + y_n + \xi_n^x + u_n^x \\ y_{n+1} &= y_n - \sigma x_n - \beta + \xi_n^y + u_n^y, \end{aligned} \tag{3}$$

where the disturbance is bounded so that $\sqrt{(\xi_n^x)^2 + (\xi_n^y)^2} \leq \xi_0$, and the control applied is also considered bounded so that $\sqrt{(u_n^x)^2 + (u_n^y)^2} \leq u_0$. To simplify the notation, we define the state vector $q_n = (x_n, y_n)$, the disturbance vector $\xi_n = (\xi_n^x, \xi_n^y)$ and the control vector $u_n = (u_n^x, u_n^y)$ so that the map given by Eq. (3) can be written as:

$$q_{n+1} = f(q_n) + \xi_n + u_n, \tag{4}$$

with $|\xi_n| \leq \xi_0$ and $|u_n| \leq u_0$. This upper control bound u_0 is specified by the controller but we have to take into account that not any u_0 value is possible. There is a minimum value u_0^{min} for which exist points in Q that are controllable. These points constitute a subset of Q that we name the set S. Higher values of $u_0 > u_0^{min}$ result in a larger set S.

The computation of the set $S \subset Q$ can be realized through a recursive algorithm. Beginning from the set $Q_0 = Q$, the points $q_n \in Q$ for which the image $f(q_n) + \xi_n + u_n$ cannot be put it back again in Q with $|u_n| \leq u_0$, are removed. Notice that, for every point q_n, all possible disturbances $|\xi_n| \leq \xi_0$ must be evaluated. If for any of these disturbances, the point cannot be controlled, then the point q_n is removed from Q_0. There is only one exception to this rule. The points $q_n \in Q_0$ for which the image $f(q_n) + \xi_n$ abandon Q_0 through the right or left boundary are not removed. This exception is required since we want the controlled orbits to pass across the region Q and leave it through the right or left boundary. In that sense we want that Q actuates like a bridge connecting the right ($y > y_3$) and the left ($y < y_2$) chaotic sides of the phase space and preventing that the orbit escapes through bottom ($x = -1.82$) boundary of Q.

After removing all the uncontrollable points $q_n \in Q_0$ in the first iteration of the algorithm, the surviving points constitutes a new subset $Q_1 \subset Q_0$. The second iteration of the algorithm consists on repeating the process described before, but with the subset Q_1 instead of Q_0. After that we obtain the subset $Q_2 \subset Q_1 \subset Q_0$. In the next steps, the algorithm is repeated until it converges, that is when $Q_{i+1} = Q_i$. This final set will be S. This set guarantees that any point $q_n \in S$ can be controlled in S applying every iteration a control $|u_n| \leq u_0$, unless the orbit abandons Q across the right or left boundaries. In that instant the applications of control is stopped.

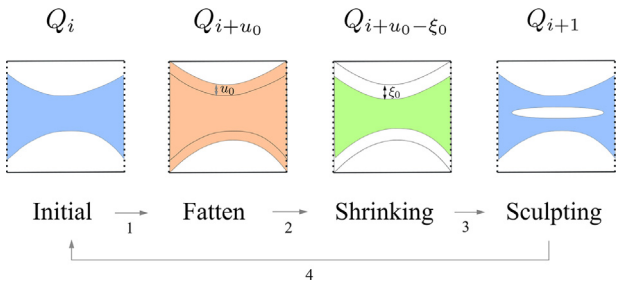

Fig. 5. Recursive algorithm to compute the set $S \subset Q$. Beginning with $Q_0 = Q$.
Step 1. Fatten the set Q_i by u_0 except the right and left boundaries, obtaining the set denoted by $(Q_i + u_0)$.
Step 2. Shrink the set $(Q_i + u_0)$ by ξ_0 except the right and left boundaries, obtaining the set denoted by $(Q_i + u_0 - \xi_0)$.
Step 3. Let Q_{i+1} be the points $q \in Q_i$, for which $f(q)$ fall inside the set denoted $(Q_i + u_0 - \xi_0)$, or the points $q \in Q_i$ for which $f(q)$ abandon Q through the right or left boundaries.
Step 4. Return to step 1, unless $Q_{i+1} = Q_i$. We call this final region, the set S.

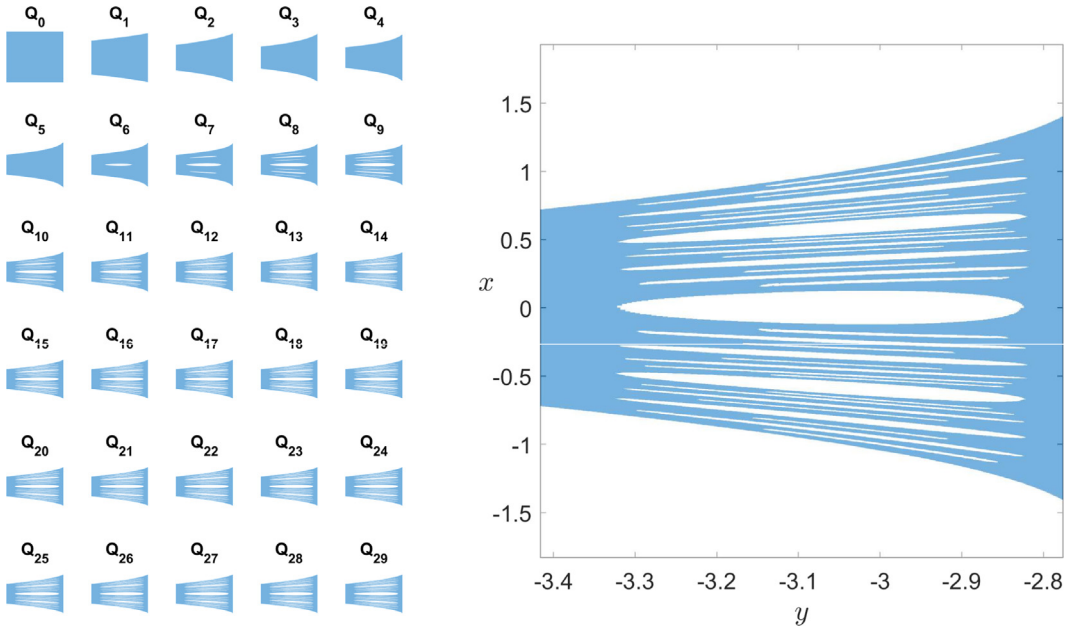

Fig. 6. Computation of the set S with $\xi_0 = 0.010$ and $u_0 = 0.008$. The region Q is taken as the rectangle $(y, x) \in [-3.42, -2.78] \times [-1.82, 1.92]$. The right and left sides of Q are open boundaries. The grid resolution taken in Q is 1000×1000 points. The computation of the set S, starting from Q_0, takes 29 iterations to converge (see the left small figures). In this case the set S corresponds to Q_{29} shown in bigger size on the right.

The computation of the set S as described above, can be greatly speeded up with the following algorithm based on morphological transformations of Q. Given the initial region $Q_0 = Q$ and the upper bounds ξ_0 and u_0, the *ith* step of the algorithm is summarized in Fig. 5.

Notice that if the value u_0 selected is too small, the final set S will be the empty set (no points in Q are controllable with such a small control) and therefore we have to select a bigger value u_0. As controllers, we want to keep the amount of control as low as possible, so it is reasonable to try to find out the minimum u_0, named u_0^{min}, for which the set S exists. To do that, we compute the set S several times, taking each time a value u_0 closer to the u_0^{min}. That is, for a given value u_0, if the set S exists, then we compute it again with a smaller value u_0. If the set S is empty, we compute it again with a bigger value u_0. In that way we can approximately find the u_0^{min}. All the sets S shown in this work were computed with a value u_0 very close to the u_0^{min} so the sets S are minimal. Any other set computed with a bigger value u_0 will contain the minimal set S.

In order to compute an example, we choose the upper disturbance bound affecting the map to be $\xi_0 = 0.010$. For this value we found that the minimum control bound for which the set S exists is approximately $u_0 = 0.008$. After applying the recursive algorithm, we obtain the set S shown in Fig. 6, where we also display the 29 iterations that the algorithm takes to converge, from Q_0 to Q_{29}. In the following subsections we describe three different scenarios that we consider of interest, where the orbit is controlled in S to extend the chaotic bursting of the neuron.

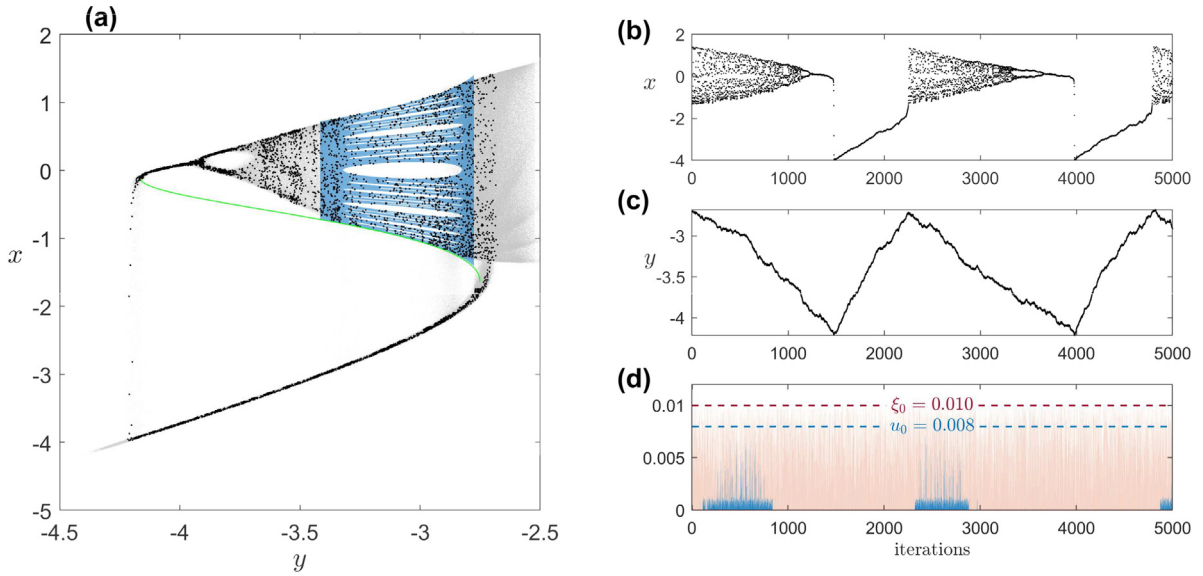

Fig. 7. Long bursting control. (a) In blue the set S computed for $\xi_0 = 0.010$ and $u_0 = 0.008$. In this set, the control is applied to the orbit (black dots) allowing it to reach the left chaotic region and thus completing a long bursting. (b) The x-time series of the controlled orbit. (c) The y-time series of the controlled orbit. (d) The disturbances $|\xi_n|$ (brown bars) affecting the orbit and the controls $|u_n|$ (blue bars) applied during the 5000 iterations of the orbit. This control never exceeds the value $u_0 = 0.008$.

4. Control implementation using the set S

In this section we use the set S computed in the previous section to control the orbits. Although the set S was computed to sustain the chaotic orbit through all the region Q, we will show that the set S can be also used to control the bursting size in Q. Here we distinguish the following three scenarios of control implementation.

4.1. Control through all the region Q (the long bursting)

In this scenario, we control the orbit in Q to allow them to achieve the left side of Q. All we have to do when the orbit enters in S is to apply every iteration of the map $q_{n+1} = f(q_n) + \xi_n + u_n$ the corresponding control $|u_n| \leq u_0 = 0.008$ to keep the orbit inside S until it escapes through the left boundary.

In Fig. 7, we show the result of controlling the orbit through all the region Q. As shown in Fig. 7(a), the bursting size is greatly increased as can be seen if we compare the x-time series shown in Fig. 7(b) and the x-time series corresponding to the uncontrolled orbit shown before in Fig. 3(b). In Fig. 7(c) and (d), we also show the y-time series and the disturbance and the control affecting the 5000 iterations of the orbit. Notice that in this scenario, the chaotic oscillations (bursting) comes with a final periodic oscillation, so that in the high activity period of the neuron, both behaviours are present.

4.2. Control until a specific y value in the set S (the y-stop).

In this subsection and the next one, we show how we can use the set S to control the bursting size of the neuron. In particular, here we analyse the possibility of stop the bursting when the orbit reaches a certain y value inside Q.

To compute an example, we choose the limiting value $y_{stop} = -3.1$ (which is inside the set Q). Once the controlled orbit reaches this value, we just cease the application of control. Next, after a short chaotic transient, the orbit naturally escapes from Q through the bottom boundary and the bursting stops. Then, the orbit returns through the stable manifold to initiate the next bursting cycle.

This simple method of stopping the bursting works well in this system. However, depending on the disturbance affecting the transient chaotic orbits, they can take different times to escape from Q. A good strategy to reduce this time is, when the orbit reaches the value $y_{stop} = -3.1$, to continue applying a control $|u_n| \leq u_0$, but now with the aim of pushing the orbit as far as possible from the set S. This approach significantly reduces the escape time of the orbit.

The result of this control is shown in Fig. 8. In Fig. 8(a) and (b), it can be appreciated that the bursting is abruptly stopped when the controlled orbit reaches the value $y = -3.1$. Then, the y variable starts to grow again, see Fig. 8(c). Note that in this case, the control is only applied in Q, first to keep the orbit in the set S, and then to accelerate the escape from it. This is clearly shown in Fig. 8(d) where the disturbance and the control applied to the orbit are also displayed.

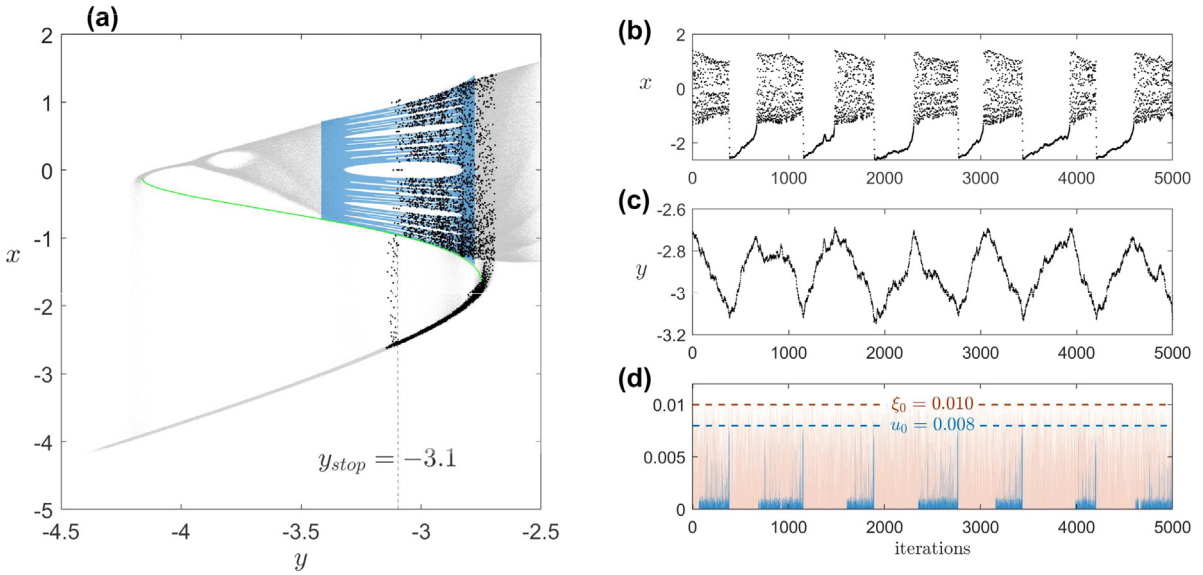

Fig. 8. Control until a specific y value in set S. (a) In blue the set S computed for $\xi_0 = 0.010$ and $u_0 = 0.008$. In this set, the control is applied to sustain the orbit (black dots) until it reaches the value $y = -3.1$. Then the escape of the orbit from S is forced. (b) The x-time series of the controlled orbit. (c) The y-time series of the controlled orbit. (d) The disturbances $|\xi_n|$ (brown bars) affecting the orbit and the controls $|u_n|$ (blue bars) applied during the 5000 iterations of the orbit. Note that the control is only applied inside Q and it never exceeds the upper bound value $u_0 = 0.008$.

In this scenario of control, it is important to stress out that the bursting cycles have different size (see Fig. 8(a)). This is mainly due to the fact that the slow variable y that leads the cycle is affected by disturbances, just as the x variable, and therefore every bursting can take a different number of iterations to reach the stopping value $y = -3.1$. The higher the upper disturbance bound, the more different bursting size we found. To achieve more similar cycles we propose an alternative control strategy in the next subsection.

4.3. Control to obtain cycles with a similar size

What we pursue here, is to obtain bursting cycles with approximately the same size. To do that, we stop the bursting regime when it reaches certain number of iterations. The only requirement is that the orbit has to be in Q. Here, as an example, we choose to stop the bursting when the bursting reaches 600 iterations. However this condition is not enough to achieve similar burstings size because the y-variable is affected by the disturbance in all the chaotic cycle, (i.e., the bursting period in Q and in the low activity period outside Q), and therefore we need to control the y-variable during all the cycle.

To do that, we assume that we know the behaviour of the map without disturbances. Taking into account that this deterministic map produces chaotic cycles with similar sizes, we can use the y-variable of this deterministic map (we call it y^*), to lead the y-variable of our map affected by disturbances. In that way we can achieve cycles with similar size.

Combining the above control of the variable y along all the cycle, and the control of both variables x and y in the region Q, and taking into account the constraint ($|u_n| \leq u_0$) in each iteration, we propose the following full scheme of control:

- For a given point q_n of the orbit, if we want that the image $q_{n+1} = f(q_n) + \xi_n + u_n$ maps in S, among all the possible points $q_{n+1} \in S$ (reachable with $|u_n| \leq u_0$) we choose the point for which $|y - y^*|$ is smaller.
- For a given point q_n of the orbit, if we want that the image $q_{n+1} = f(q_n) + \xi_n + u_n$ maps outside S, among all the possible points $q_{n+1} \notin S$ (reachable with $|u_n| \leq u_0$) we choose the point for which $|y - y^*|$ is smaller.

The result of this control scheme is shown in Fig. 9(a). This figure is very similar to Fig. 8(a), nevertheless it should be noticed that in this case, the bursting is stopped when the bursting duration reaches 600 iterations, instead of stopping when the orbit reaches the value $y = -3.1$. Furthermore, as a result of controlling the y-variable all the time, the resulting cycles have approximately the same size as shown in Fig. 9(b). See also that the y-series of the controlled orbit, Fig. 9(c), is much more smooth than the y-series presented in Fig. 8(c). The counterpart of this control scheme is that now, the amount of control used is larger (see Fig. 9(d)) but always below the upper control bound $u_0 = 0.008$.

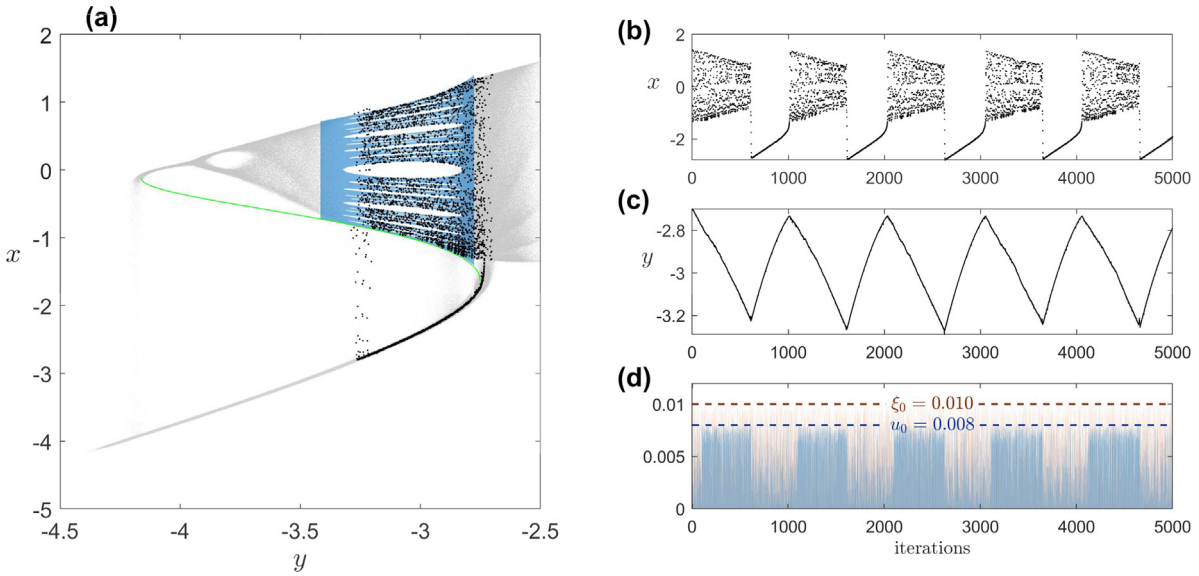

Fig. 9. Control to obtain cycles with similar size. (a) In blue the set S computed for $\xi_0 = 0.010$ and $u_0 = 0.008$. In this set, the control is applied to sustain the orbit (black dots) in the safe set until it reaches 600 iterations in the bursting regime. Then the escape of the orbit from the safe set is forced. In this way, we can control exactly the duration of the bursting. (b) The x-time series of the controlled orbit. (c) The y-time series of the controlled orbit. (d) The disturbances $|\xi_n|$ (brown bars) affecting the orbit and the controls $|u_n|$ (blue bars) applied during the 5000 iterations of the orbit.

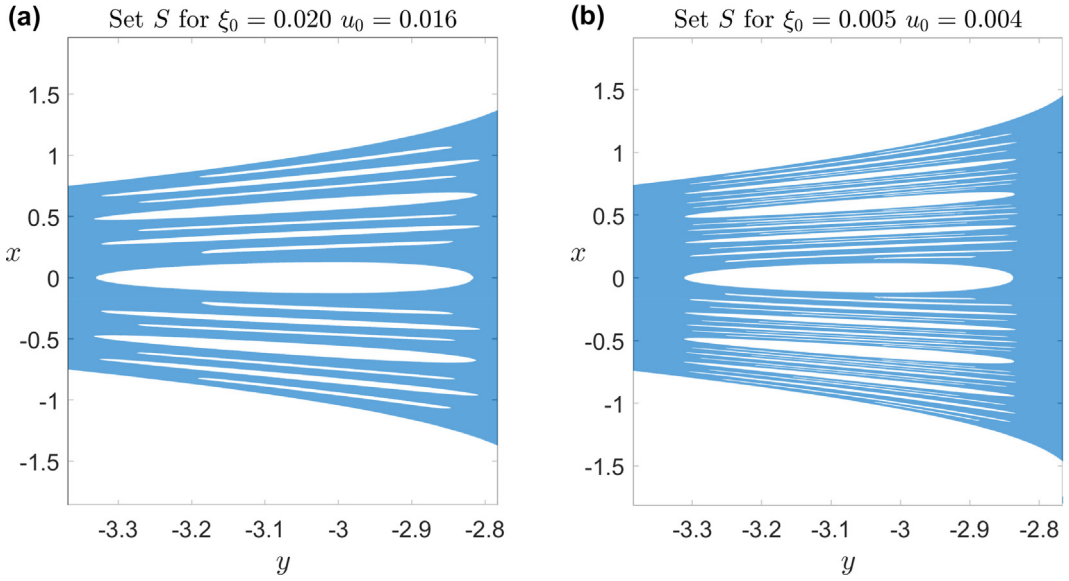

Fig. 10. Computing the set S for different values ξ_0. In both cases the region Q is taken as the rectangle $(y, x) \in [-3.42, -2.78] \times [-1.82, 1.92]$. The right and left sides of Q are open boundaries. The grid resolution taken in Q is 2000×2000 points. (a) The set S computed for $\xi_0 = 0.020$ and $u_0 = 0.016$. It takes 23 iterations to converges. (b) The set S computed for $\xi_0 = 0.005$ and $u_0 = 0.004$. Note the finer structure for smaller values of ξ_0. It takes 37 iterations to converges.

5. Sets S for different values of the disturbance ξ_0

In the previous section we have shown the application of the control in three different scenarios where we use the upper disturbance bound $\xi_0 = 0.010$ and the upper control bound $u_0 = 0.008$. However, if the values ξ_0 and u_0 are different, the set S will be different, as shown in Fig. 10. In order to show how this change affects the controlled orbits, we compute again the three scenarios presented before, but for a different disturbance value ξ_0 affecting the map. In one case we choose a bigger disturbance $\xi_0 = 0.020$ and in the other one, a smaller disturbance $\xi_0 = 0.005$.

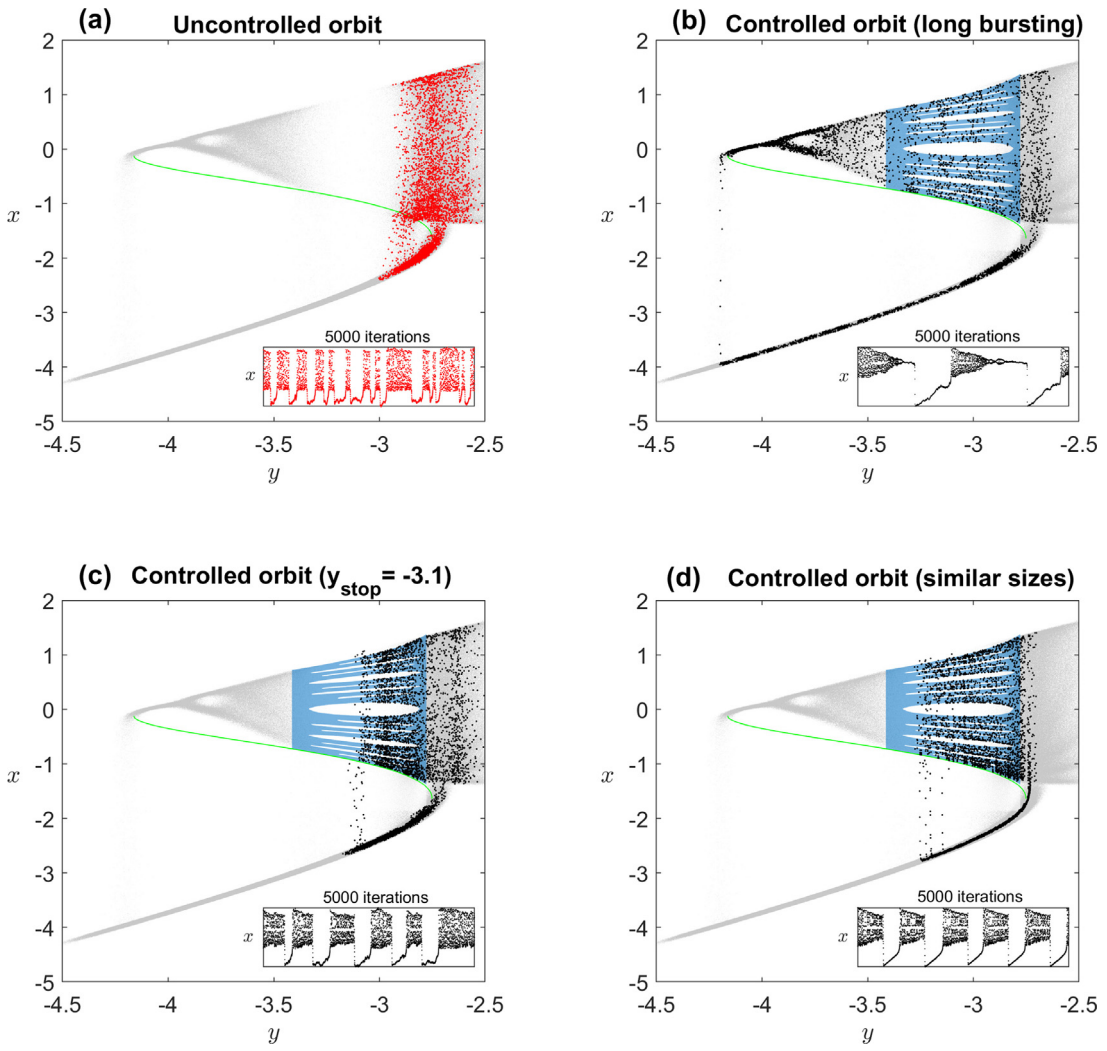

Fig. 11. Big disturbance. Controlling orbits with $\xi_0 = 0.020$ and $u_0 = 0.016$. Controlled orbits corresponding to the three scenarios presented in Section 4. The only change is the bigger disturbance ξ_0 affecting the map and therefore the bigger control u_0 required. (a) Uncontrolled orbit. (b) Long bursting size. (c) Control until a specific y value in the set S. (d) Control to obtain cycles with similar size. The bursting size selected is 600 iterations.

For the case $\xi_0 = 0.020$, we obtain that the minimum upper control bound for which the set S exists is $u_0 = 0.016$ (see Fig. 10(a)) . The corresponding controlled orbits for the three scenarios are shown in Fig. 11.

In the other case, we assume that the upper disturbance bound affecting the map is $\xi_0 = 0.005$. The minimum upper control bound for which the set S exists is $u_0 = 0.004$ (see Fig. 10(b)). The corresponding controlled orbits for the three scenarios are shown in Fig. 12.

These two examples, where different ξ_0 have been chosen, reveal the most important feature of the control method. Not only it takes into account the random disturbance affecting the system, but also its intensity, obtaining different sets S that minimize the necessary control in each case.

6. Disturbances and control in only one variable.

Along this work we have used the following Rulkov map model:

$$\begin{aligned} x_{n+1} &= \frac{\alpha}{(1+x_n^2)} + y_n + \xi_n^x + u_n^x \\ y_{n+1} &= y_n - \sigma x_n - \beta + \xi_n^y + u_n^y, \end{aligned} \tag{5}$$

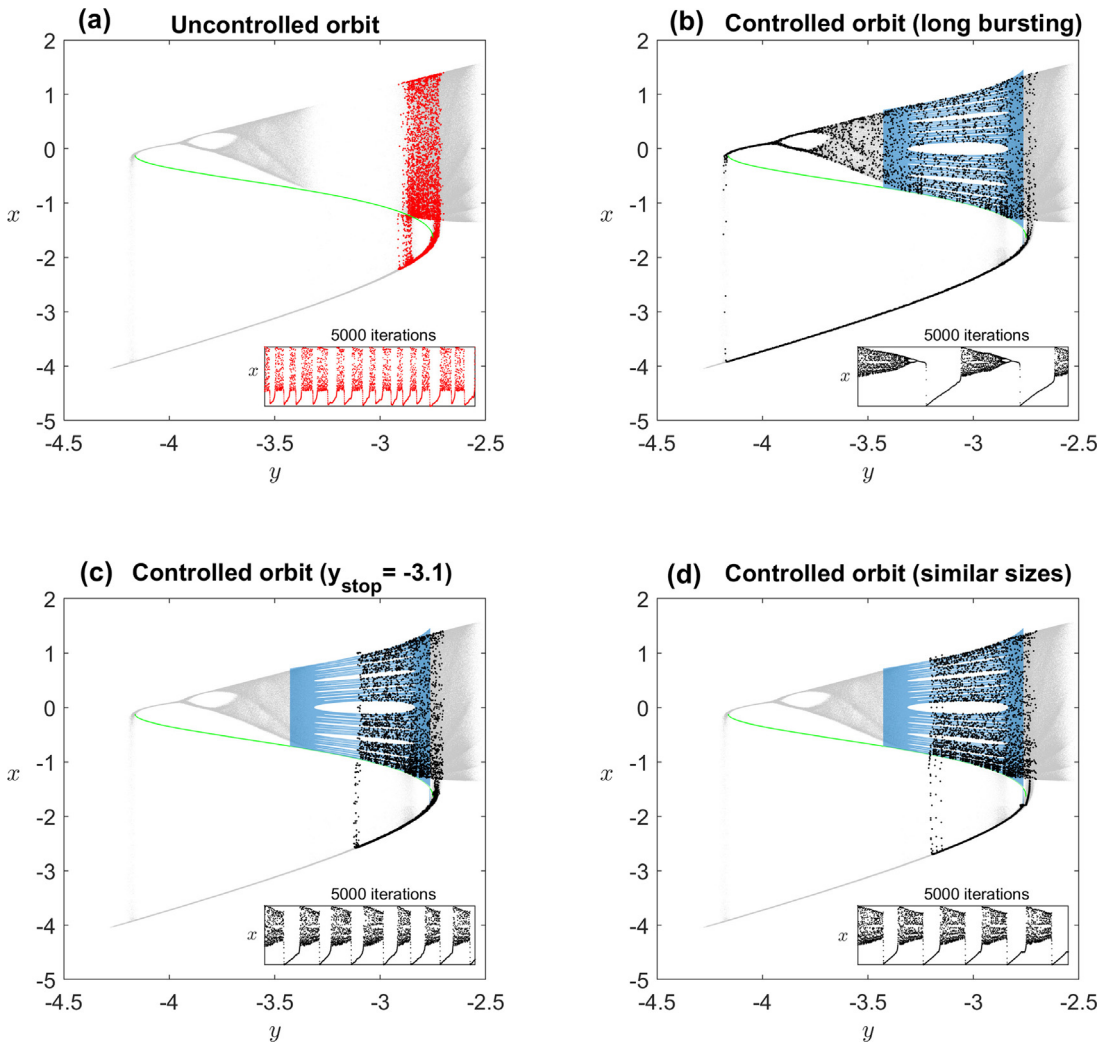

Fig. 12. Small disturbance. Controlling orbits with $\xi_0 = 0.005$ and $u_0 = 0.004$. Controlled orbits corresponding to the three scenarios presented in Section 4. The only change is the smaller disturbance ξ_0 affecting the map and therefore the smaller control u_0 required. (a) Uncontrolled orbit. (b) Long bursting size. (c) Control until a specific y value in the set S. (d) Control to obtain cycles with similar size. The bursting size selected is 600 iterations.

where we consider that both variables were affected by disturbances and both variables can be controlled. However, to complete our study we report here a brief analysis when either one variable is not controlled or is not affected by the disturbances. The results that we obtain, can be summarized in the following three cases.

Case (a) $\xi_n^x \neq 0$, $u_n^x \neq 0$, $\xi_n^y \neq 0$, $u_n^y = 0$. If we observe the sets S computed before, they are made of approximately horizontal stripes. Typically, the orbit jumps from one stripe to another until it falls outside S. In that moment, the control is applied to return the orbit back to the nearest stripe. Due to the horizontal distribution of the stripes, the control applied is mainly in the vertical axis (x-axis). For this reason, if we compute the set S allowing only control in the variable x, the set S that we obtain is very similar to the ones computed in the previous sections. The only difference is that the minimum value u_0^{min} for which the set S exists, it is slightly larger than the u_0^{min} obtained when the control is allowed in both variables. For example, in the set S computed in Section 3 we obtain a $u_0^{min} = 0.008$, while in the case of $u_n^y = 0$, we have obtain $u_0^{min} = 0.0085$.

Case (b) $\xi_n^x \neq 0$, $u_n^x \neq 0$, $\xi_n^y = 0$, $u_n^y = 0$. The sets S that we obtain in this case are very similar with the sets S shown in this work. The reasons are the same as explained in the previous case, the control u_n^x is active. However there is an important change. Due to the absence of disturbance in the slow-variable y, the control scheme proposed in the scenario three to get cycles with similar size is not needed since the y-variable behaves smoothly. Even though we know that the disturbance affecting the x-variable, will affects the y-variable in the next iteration of the map, the

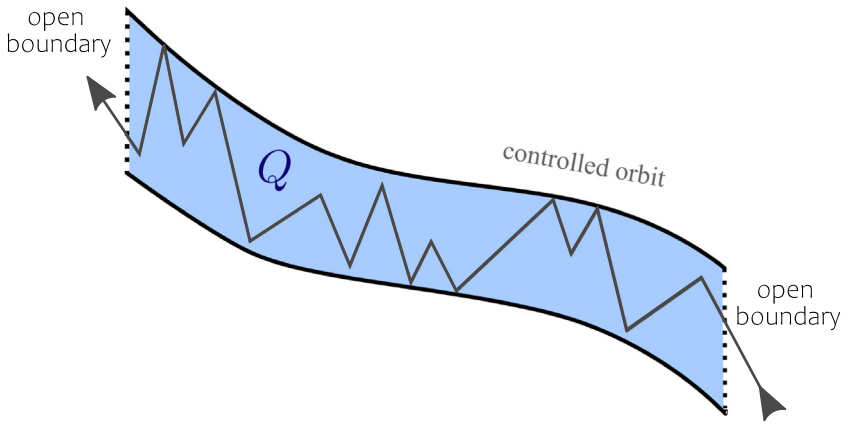

Fig. 13. Schematic control goal. The region Q, depicted in blue, is defined in the phase space for the purpose of connecting different regions within the phase space.

influence of this disturbance is very small due to the small coupling value $\sigma = 0.001$ in the equations. As a result, the y-variable behaves almost as deterministic and therefore the bursting sizes obtained in both, the scenario two and three, are very similar.

Case (c) $\xi_n^x \neq 0$, $u_n^x = 0$, $\xi_n^y \neq 0$, $u_n^y \neq 0$. If we try to compute sets S controlling only the y-variable, we found that it is necessary to apply a very big control resulting in a big u_0^{min} value. Since the y-variable is the slow variable, to apply a big control on it will completely destroy the bursting behaviour of the cycles, and for that reason we consider this case (for this map) of no interest, since we want to preserve the chaotic behaviour of the neuron.

7. Generalization of the control method

The control method described in this work has been designed to extend and control the bursting size of a neuron that behaves according to the Rulkov map, Eq. (2). For this case, we define a region Q where the orbits are allowed to enter or abandon it across the right or left boundaries, but not across the top or bottom boundaries. In this way, we were able to extend the bursting size of the neuron.

There might be other systems where the applications of this control scheme can be useful. In general, given a system, we can design a region Q in the phase space, that actuates like a bridge (see Fig. 13) for the orbits to connect regions of the phase space that otherwise would be impossible .

The steps to apply this control technique is summarized as follows:

- Define the region Q in the phase space to connect different regions of phase space. We assume that the dynamics in Q can be described as $q_{n+1} = f(q_n) + \xi_n + u_n$, with $|\xi_n| \leq \xi_0$ and $|u_n| \leq u_0$.
- Define the boundaries behaviour (open or close). Orbits are allowed to escape/enter in Q through the open boundaries. Orbits are not allow to escape/enter in Q through the closed boundaries.
- Apply the following recursive algorithm. Beginning with $Q_0 = Q$. The ith iteration of the algorithm is:

    1. Fatten the set Q_i by u_0 except the open boundaries, obtaining the set denoted by $(Q_i + u_0)$.
    2. Shrink the set $Q_i + u_0$ by ξ_0 except the open boundaries, obtaining the set denoted by $(Q_i + u_0 - \xi_0)$.
    3. Let Q_{i+1} be the points $q \in Q_i$, for which $f(q)$ falls inside the set denoted $(Q_i + u_0 - \xi_0)$, or the points $q \in Q_i$ for which $f(q)$ abandon Q through an open boundaries.
    4. Return to step 1, unless $Q_{i+1} = Q_i$. We call this final set, the set S.

- Control the orbits with the set S. Given a point $q \in S$, we evaluate $f(q_n) + \xi_n$ and then we apply the corresponding control $|u_n| \leq u_0$ to put the orbit back in S unless $f(q_n) + \xi_n$ escapes from Q through an open boundary.

Here we want to point out three important considerations. First, this control scheme only describes how an orbit is controlled in the set $S \in Q$. The way the orbit enters in S should be taken into account to design an appropriate region Q in the phase space. For example, in the case of the Rulkov map (see Fig. 4), if we take a bad region Q' as the rectangle $(y, x) \in [-3.5, -3] \times [-1.82, 1.92]$ that does not touch the left chaotic region, most of the orbits, after a short chaotic transient, will fall towards the stable manifold at the bottom, and never reaches the right boundary ($y = -3$) of Q'. In consequence, very few orbits will enter in Q'.

Second, the condition that we establish for the open boundaries (orbits can enter/escape through this boundary), is not well defined since we are working with maps (discrete trajectories) not with flows (continuous trajectories). The criterion that we follow in this work is the simplest one. For a given orbit such that q_n is in Q and q_{n+1} maps outside Q, we draw an imaginary straight line between q_n and q_{n+1}. If the line crosses the open boundary, we consider that the orbit is abandon Q through the open boundary. If not, we apply the corresponding control $|u_n| \leq u_0$ to put the orbit back in Q. This is only one criterion among all the possible choices to define if an orbit crosses an open boundary, and the controller is free to set his own criterion. The steps of the recursive algorithm to obtain S applies in the same way.

Third, this control scheme is designed to be minimally invasive. The control is not applied to guide the orbit from one open boundary to another open boundary. The control scheme is applied to sustain the orbit in Q until, if it happens, the orbit escapes across one of the open boundaries. However, as we show in Section 4.3 this control technique can be combined with an additional control as long as the controls applied satisfies $|u_n| \leq u_0$.

8. Conclusions

In this work, we propose a control technique that allows orbits on a map to connect different regions of the phase space, that otherwise would be isolated. The control method is applied on maps in which we assume that some of the variables can be controlled. In particular, we have shown the applications of this method in the dynamics of a neuron modelled by the two-dimensional Rulkov map, for a choice of parameters where chaotic burstings are present. The goal of the control is to extend the bursting size of the neuron applying tiny controls on the variables, that we also consider affected by bounded disturbances (bounded noise). The modification of the bursting size is noteworthy because it has been shown that plays a critical role in the encoding and transmission of specific information and for the operation of the central pattern generators (CPGs), responsible for essential rhythmic behaviours such as walking or breathing.

To apply the method, we define a region Q in the phase space between two separated chaotic regions. To connect both chaotic regions and allow the orbits to exhibit long bursting, we compute a special subset $S \subset Q$ where the orbits can be sustained with a minimal control. Once the set S is obtained, we consider three scenarios of application.

In the first scenario, the control is applied in all the set S to lead the orbit from one chaotic region to the other, resulting in a long bursting size. In the second scenario, we stop the bursting when the orbit reaches a predefined y-value in Q resulting in shorter bursting sizes. In the third scenario we stop the bursting when it reaches a certain number of iterations. In addition, in this last case, we add an extra control in the y-variable to achieve similar cycles with approximately the same bursting size. In all the scenarios, we show how the S adapts for different disturbance bound to minimize the control bound necessary to sustain the orbits in Q.

After that, we report the case in which only one variable is controlled showing that the control in the x-variable is necessary to keep the chaotic behaviour of the neuron. Finally, we have explained the generalization of the method, in case of its potential application to other systems.

CRediT authorship contribution statement

Jennifer López: Software, Investigation. **Mattia Coccolo:** conceptualization, Software, Investigation, Writing – original draft, writing – review & editing, Supervision. **Rubén Capeáns:** conceptualization, Software, Investigation, Writing – original draft, Writing – review & editing, Supervision, Methodology. **Miguel A.F. Sanjuán:** Writing – original draft, Writing – review & editing, Supervision, Project administration, Funding acquisition.

Declaration of competing interest

The authors declare that they have no known competing financial interests or personal relationships that could have appeared to influence the work reported in this paper.

Data availability

No data was used for the research described in the article.

Acknowledgements

This work has been supported by the Spanish State Research Agency (AEI) and the European Regional Development Fund (ERDF, EU) under Project No. PID2019-105554GB-I00 (MCIN/AEI/10.13039/501100011033).

References

[1] Rocsoreanu C, Georgescu A, Giurgiteanu N. The fitzhugh–nagumo model: Bifurcation and dynamics. Dordrecht, Netherlands: Springer; 2000.
[2] González-Mir JM. Complex bifurcation structures in the Hindmarsh–Rose neuron model. Int J Bifurcation Chaos 2007;17:3071–83.
[3] Guckenheimer J, Oliva RA. Chaos in the Hodgkin–Huxley model. SIAM J Appl Dyn Syst 2002;1:105–14.
[4] Ibarz B, Casado JM, Sanjuán MAF. Map-based models in neuronal dynamics. Phys Rep 2011;501:1–74.
[5] Rulkov NF. Regularization of synchronized chaotic bursts. Phys Rev Lett 2001;86:183.
[6] Bashkirtseva I, Ryashko L. Analysis of noise-induced chaos-order transitions in Rulkov model near crisis bifurcations. Int J Bifurcation Chaos 2017;27:1730014.
[7] Bashkirtseva I, Nasyrova V, Ryashko L. Noise-induced bursting and chaos in the two-dimensional Rulkov model. Chaos Solitons Fractals 2018;110:76–81.
[8] Bashkirtseva I. Stochastic phenomena in one-dimensional Rulkov model of neuronal dynamics. Discrete Dyn Nat Soc 2015;2015.
[9] Wang C, Cao H. Parameter space of the Rulkov chaotic neuron model. Commun Nonlinear Sci Numer Simul 2014;19:2060–70.
[10] Lozano R, Sanjuán MAF. Fourier analysis of a delayed Rulkov neuron network. Commun Nonlinear Sci Numer Simul 2019;75:62–75.
[11] Wang C, Cao H. Stability and chaos of Rulkov map-based neuron network with electrical synapse. Commun Nonlinear Sci Numer Simul 2015;20:536–45.
[12] Zeldenrust F, Wadman WJ, Englitz B. Neural coding with bursts—current state and future perspectives. Front Comput Neurosci 2018;12:48.
[13] Kepecs A, Lisman J. How to read a burst duration code. Neurocomputing 2004;58:1–6.
[14] Marder E, Bucher D. Central pattern generators and the control of rhythmic movements. Curr Biol 2001;11(23):R986–96.
[15] Kepecs A, Wang XJ, Lisman J. Bursting neurons signal input slope. J Neurosci 2002;22(20):9053–62.
[16] Shao J, Liu Y, Gao D, Tu J, Yang F. Neural burst firing and its roles in mental and neurological disorders. Front Cell Neurosci 2021;15.
[17] Prince DA. Neurophysiology of epilepsy. Annu Rev Neurosci 1978;1(1):395–415.
[18] Yang H, Gong P, Jiao X, Zhou Q, Zhang Y, Jiang Y, Yang Z. The relationship between the characteristics of burst suppression pattern and different etiologies in epilepsy. Sci Rep 2021;11(1):1–8.
[19] Sabuco J, Zambrano S, Sanjuán MAF, Yorke JA. Finding safety in partially controllable chaotic systems. Commun Nonlinear Sci Numer Simul 2012;17:4274–80.
[20] Capeáns R, Sabuco J, Sanjuán MAF, Yorke JA. Partially controlling transient chaos in the Lorenz equations. Philos Trans R Soc A 2016;375:20160211.
[21] Capeáns R, Sabuco J, Sanjuán MAF. Partial control of chaos: How to avoid undesirable behaviors with small controls in presence of noise. Discrete Contin Dyn Syst B 2018;23:3237–74.
[22] Capeáns R, Sanjuán MAF. Partial control of delay-coordinate maps. Nonlinear Dyn 2018;92:1419–29.
[23] Coccolo M, Seoane JM, Zambrano S, Sanjuán MAF. Partial control of escapes in chaotic scattering. Int J Bifurcation Chaos 2013;23:1350008.
[24] Capeáns R, Sabuco J, Sanjuán MAF. A new approach of the partial control method in chaotic systems. Nonlinear Dyn 2019;98:873–87.
[25] Capeáns R, Sanjuán MAF. Beyond partial control: controlling chaotic transients with the safety function. Nonlinear Dyn 2022;107:2903–10.
[26] Rulkov NF. Modeling of spiking–bursting neural behavior using two-dimensional map. Phys Rev E 2002;65:041922.
[27] Lindner B, García-Ojalvo J, Neiman A, Schimansky-Geier L. Effects of noise in excitable systems. Phys Rep 2004;392:321–424.
[28] Hilborn RC. A simple model for stochastic coherence and stochastic resonance. Amer J Phys 2004;72:528–33.
[29] Hilborn RC, Erwin RJ. Fokker–Planck analysis of stochastic coherence in models of an excitable neuron with noise in both fast and slow dynamics. Phys Rev E 2005;72:031112.
[30] Hilborn RC, Erwin RJ. Coherence resonance in models of an excitable neuron with noise in both the fast and slow dynamics. Phys Lett A 2004;322:19–24.